

Deep Learning of ab initio Hessians for Transition State Optimization

Eric C.-Y. Yuan^{*1,3}, Anup Kumar^{*4}, Xingyi Guan^{1,3}, Eric D. Hermes⁵, Andrew S. Rosen^{6,7},
Judit Zádor⁸, Teresa Head-Gordon¹⁻³, Samuel M. Blau⁴

¹Kenneth S. Pitzer Theory Center and Department of Chemistry,

²Departments of Bioengineering and Chemical and Biomolecular Engineering,
University of California, Berkeley, CA, 94720 USA

³Chemical Sciences Division, Lawrence Berkeley National Laboratory, Berkeley, CA, 94720 USA

⁴Energy Technologies Area, Lawrence Berkeley National Laboratory, Berkeley, CA, 94720 USA

⁵Quantum-Si, Branford, CT, 06405 USA

⁶Materials Sciences Division, Lawrence Berkeley National Laboratory, Berkeley, CA, 94720 USA

⁷Department of Materials Science and Engineering, University of California, Berkeley, CA 94720, USA

⁸Combustion Research Facility, Sandia National Laboratories, Livermore, CA, 94550, USA

*Authors contributed equally

Corresponding authors: thg@berkeley.edu, smblau@lbl.gov

Abstract

Identifying transition states – saddle points on the potential energy surface connecting reactant and product minima – is central to predicting kinetic barriers and understanding chemical reaction mechanisms. In this work, we train an equivariant neural network potential, NewtonNet, on an ab initio dataset of thousands of organic reactions from which we derive the analytical Hessians from the fully differentiable machine learning (ML) model. By reducing the computational cost by several orders of magnitude relative to the Density Functional Theory (DFT) ab initio source, we can afford to use the learned Hessians at every step for the saddle point optimizations. We have implemented our ML Hessian algorithm in Sella, an open source software package designed to optimize atomic systems to find saddle point structures, in order to compare transition state optimization against quasi-Newton Hessian updates using DFT or the ML model. We show that the full ML Hessian robustly finds the transition states of 240 unseen organic reactions, even when the quality of the initial guess structures are degraded, while reducing the number of optimization steps to convergence by 2–3× compared to the quasi-Newton DFT and ML methods. All data generation, NewtonNet model, and ML transition state finding methods are available in an automated workflow.

1 Introduction

Computational identification of transition states (TSs) on the quantum mechanical potential energy surface (PES) is central to predicting reaction barriers and understanding chemical reactivity.^{1,2} The height of the barrier exponentially impacts the reaction rate coefficient via the Eyring equation, and the geometric character of the metastable state is informative about the kinetic mechanism, making TSs key to describing a broad range of chemical kinetic outcomes for enzymes, next-generation synthetic catalysts, batteries, and conformational changes of molecules and materials.

Transition states are first-order saddle points, and locating them via mathematical optimization is particularly challenging on high dimensional PESs relevant in complex molecular systems. Locating an

equilibrium geometry, i.e., a local minimum on the PES, can be found using bracketing methods based on function evaluations (0th order)^{3,4} and with methods that use gradient information, such as steepest descent⁵ or conjugate gradient⁶ (1st order). Under the quadratic approximation, identification of the transition state can be more robustly achieved in fewer steps by 2nd order methods⁷ using the Hessian matrix, whose elements H_{ij} are defined as the second derivative of the energy E with respect to atomic positions R_i and R_j . However, a metastable first-order saddle point is characterized by a single negative Hessian eigenvalue, and hence 2nd order methods are indispensable to optimize for molecular TS energies and geometries.¹ The Newton-Raphson (NR) method and its variants, including restricted and augmented methods like the trust radius method (TRM) and the rational function optimization (RFO) method, select the displacement vector $\Delta R^{(k)}$ (or in internal coordinates) at step k using the inverse Hessian $[H^{(k)}]^{-1}$ and the gradient $g^{(k)}$.⁸⁻¹⁰ The geometry direct inversion of the iterative subspaces (GDIIS) method and its variants similarly utilize Hessians and gradients to define a search space for optimization.¹¹

However, the evaluation of analytical Hessians for ab initio methods such as Density Functional Theory (DFT) requires solving coupled-perturbed equations, which scales one power of system size N higher than the energy or the gradient and thus can be prohibitively expensive. Consequently, several TS optimization approaches have been proposed that construct cheaper approximate Hessians using only gradient information to avoid expensive Hessian calculations, in general referred to as quasi-Newton (QN) methods.¹²⁻¹⁸ Arguably the most widely used Hessian approximation for minimization is arguably the Broyden-Fletcher-Goldfarb-Shanno (BFGS) method, where the Hessian is iteratively updated using a rank-2 matrix generated from the displacements and gradients. Such Hessian updates, however, are positive definite by design and thus cannot be applied to TS searches. Instead, methods such as symmetric rank-one (SR1) or Murtagh-Sargent,¹⁹ Powell-symmetric-Broyden (PSB), Murtagh-Sargent-Powell (MSP), Bofill, and TS-BFGS methods are developed for an indefinite approximate Hessian.²⁰⁻²⁴ On a complex PES, an optimization step can displace the molecule from the preceding quadratic region such that the resulting updated approximate Hessian quickly diverges from the true one and thus requires expensive reconstruction.¹⁰ Alternatively, double- and single-ended interpolation methods such as nudged elastic band (NEB),^{25,26} quadratic synchronous transit (QST),²⁷ and growing string method (GSM)²⁸ have been well-established in the field in the past few decades, and are often combined with QN updates. Despite all these efforts, TS optimization still requires significant user involvement and relies on trial and error when robust Hessian information is absent. However, if the full Hessian is available at every optimization step, concerns regarding the quality of the initial Hessian and subsequent updates become much less of a problem when determining a TS.

The recent development of deep learning models for the PES provides a whole new possibility for acquiring and applying the Hessian in chemically relevant tasks.²⁹⁻³³ Intuitively, the power of a fully differentiable machine learning (ML) force field does not stop at forces or gradients but also broadly applies to second (and higher order) derivative properties such as the Hessian matrix H_{ij} . In this case, it is possible to calculate Hessians analytically by automatic differentiation, by finite differences using gradients from the machine learning model, or by estimating Hessians using first order information as per the Davidson procedure.¹ For example, such an idea has recently been explored using Gaussian process regression, where an ML PES was locally trained on semiempirical energies, forces, and optionally Hessians and used to estimate the updated Hessians.^{34,35} Yet, the high memory demand using kernel-based methods can significantly reduce the applicability on all but small systems, and the semi-empirical level of theory can be deficient for reliable chemistry.

In this work, we train an equivariant message-passing neural network (eMPNN), NewtonNet,³¹ on an augmented version of the Transition-1X (T1x) dataset,³⁶ a new benchmark dataset containing ~ 10 million configurations generated by the NEB method on ~ 10 thousand gas-phase organic reactions evaluated with DFT. Although the full training data is comprised of only energies and gradients of the molecular configurations, with no Hessians provided, the whole neural network is fully differentiable such that we can

generate the Hessian H_{ij} through back propagation. We then apply the ML Hessians to TS optimization on an independent data set of 240 organic reactions previously proposed by Hermes and co-workers,^{37,38} and which are outside of the training set. We have adapted the Sella code³⁸ to read in full ML Hessians to perform TS optimizations for these reactions and utilize the same code and optimization settings in order to compare against QN Hessian optimization with either ML or DFT.

We find that incorporating explicit Hessians from the NewtonNet ML model into TS optimization yields a 2–3 \times reduction in search steps compared to approximate Hessian methods, demonstrating a remarkable efficiency improvement by ensuring higher-confidence search directions that are closer to the optimal path. The more accurate description of the Hessian also leads to improved robustness against structural perturbation such that the TS optimization is less reliant on a good initial guess. With our deep learning model, the Hessian calculation is over 1000 \times faster than the corresponding ab initio calculation and is consistently more robust in finding TSs than quasi-Newton methods using the ML or DFT potential energy surface. The combination of greater efficiency, reduced reliance on good initial guesses, and robust TS convergence for unseen reactions unveils a new realm of opportunities to utilize full Hessians for TS optimizations with appropriately constructed data sets of complex reactive chemistry.

2 Results

2.1 Machine Learned Prediction of DFT Hessians

Figure 1(a) shows the NewtonNet eMPNN model in which the DFT-computed molecular energy E is predicted by transforming and aggregating atomic features a_i that accumulate local chemical environmental information from spatial neighbors a_j and interatomic distances R_{ij} through message passing layers.³¹ The molecular energy E is then differentiated with respect to the atomic positions R_i to predict atomic forces F_i or gradients g_i , but of relevance here is that it can be auto-differentiated twice to obtain H_{ij} . We have demonstrated that the energies and forces can be predicted with excellent accuracy across a whole range of chemistry including small organic molecules³¹ as well as for methane and hydrogen combustion, even with a limited amount of training examples.^{31,39}

Like all ML potentials, the quality of the learned PES and its derivative properties depends on the availability of relevant training data. Our ML model is pre-trained on the ANI-1 dataset, which contains more than 20 million off-equilibrium conformations of small organic molecules up to 8 heavy atoms and is evaluated with the ω B97X density functional⁴⁰ and 6-31G* basis set.⁴¹ Figure 1(b) demonstrates that the original ANI-1 dataset is mostly composed of near-equilibrium geometries^{41,42} and that the reaction pathways are notably undersampled around the metastable states of the reactions.³⁶ As a result, the pre-trained ML model predicts the energies and forces accurately (with respect to the underlying DFT data) at the reactant and product states but fails significantly around the TS (Figure 1(c,d)).

Hence, it is fortunate to have the T1x dataset,³⁶ which is a new benchmark for TS-related ML tasks, containing 9,644,740 molecular configurations generated by NEB from 10,073 organic reactions, at a level of DFT commensurate with the ANI-1 data. This new data better represents the entire reaction pathway as seen in Figure 1(b) and allows us to fine-tune the pre-trained model. As seen in Figure 1(c,d) when using the fine-tuned model, the reaction barrier is more smoothly interpolated between NEB images, the false identification of an energy maximum has been eliminated, and the atomic forces are correctly predicted to be negligible as expected of a first-order saddle point.

Due to the high cost of the Hessian calculation and storage, the training datasets we use do not contain ab initio Hessian reference samples. Despite the lack of such training examples, a prediction of the atomic forces from an ML model that is continuous and smooth strongly suggests the possibility of achieving Hessian predictions without explicit training on such tasks. Based on this assumption, one approach is a finite-difference Hessian estimation that can be easily realized using the gradients predicted by our model

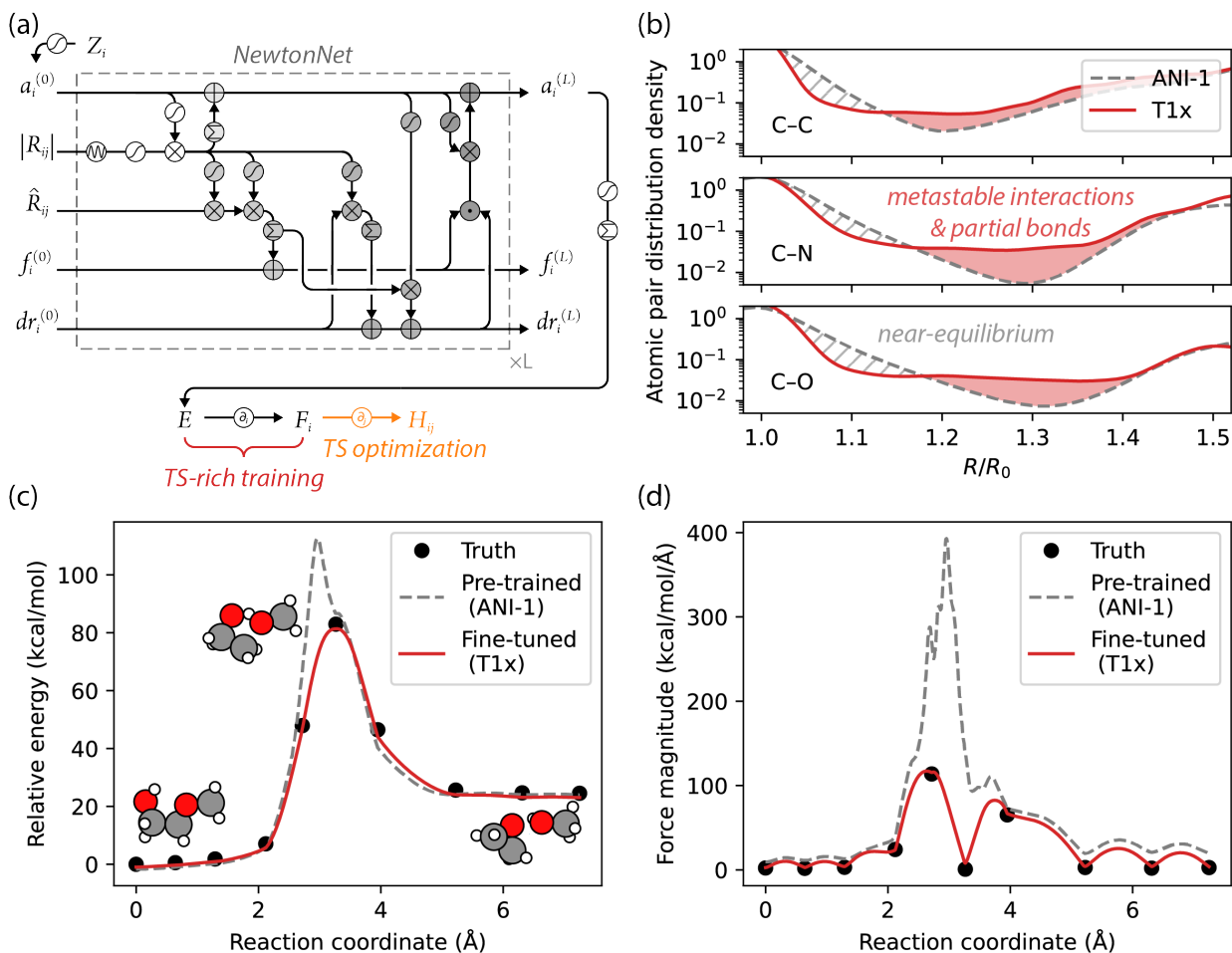


Figure 1: The *NewtonNet* model and its performance on the ANI-1 and T1-x data sets. (a) the eMPNN designed for 3D molecular graphs with nodes $\{Z_i\}$ and edges $\{R_{ij}\}$ to predict molecular energies E and atomic forces F_i .³¹ In this work, we further differentiate the network to derive $H_{i,j}$ for TS optimization tasks. (b) The distribution of atomic pairwise distances, R , relative to equilibrium bond distances, R_0 , among datasets we used for training, where the T1x data set provides more data in the TS region, and further augmented with the ANI-1x data to add data corresponding to bond compression. The predicted (c) potential energies and (d) forces along the reaction coordinate for an unseen reaction for the pre-trained and fine-tuned model. A comprehensive statistical analysis of energy and force prediction errors along the reaction coordinates for 1248 unseen test reactions is summarized in Supplementary Fig. S1 for the pre-trained and fine-tuned models. Details of the training protocols are described in Methods and Supplementary Fig. S2 and S3.

by stepping along each Cartesian axis. However, an analytical gradient of the first derivative is more cost-effective than a finite-difference method, and such a gradient can be performed as long as the neural network is at least twice differentiable. In this regard, the *NewtonNet* model is designed using sigmoid linear unit (SiLU)⁴³ and a polynomial cutoff function⁴⁴ and is therefore C^2 continuous. Utilizing the automatic differentiation in our neural network, the forces and Hessians can be analytically acquired by back propagation.

Leveraging the smoothness of the deep learning PES after fine-tuning, Figure 2 shows that reasonably accurate Hessian predictions of the reference DFT model can be acquired on molecular TSs when compared to the pre-trained model. The root mean square error (RMSE) of the predictions of eigenvalues is quantitatively quite good given the range of negative to positive values, and the eigenvector similarity between the ML and DFT models also improves significantly after fine-tuning the ML model with additional

T1x data. It is worth noting that the majority of the error arises from the positive eigenspace with a constant 20% underestimation of Hessian eigenvalues from DFT. This can be understood in part from Figure 1(b) that the T1x dataset we use for training is biased toward weaker bond and greater anharmonicity, such that lower apparent bond strength and force constants will be observed and modeled. We therefore augmented the T1x dataset by selecting 1,232,469 molecules from the ANI-1x dataset⁴² that share the same chemical formula with the T1x dataset but that exhibit compressed chemical bonds, which further improves accuracy of the Hessian predictions (Figure 1(c)). We note that some of this improvement may simply be due to the addition of more data, but it does alleviate some of the underprediction of the positive eigenvalues. Most importantly, the predicted Hessians by our fine-tuned model using the aug-T1x data have very accurate leftmost eigenvalue and eigenvector, which are the most critical ingredients in TS optimization and iterative Hessian diagonalization.^{10,45}

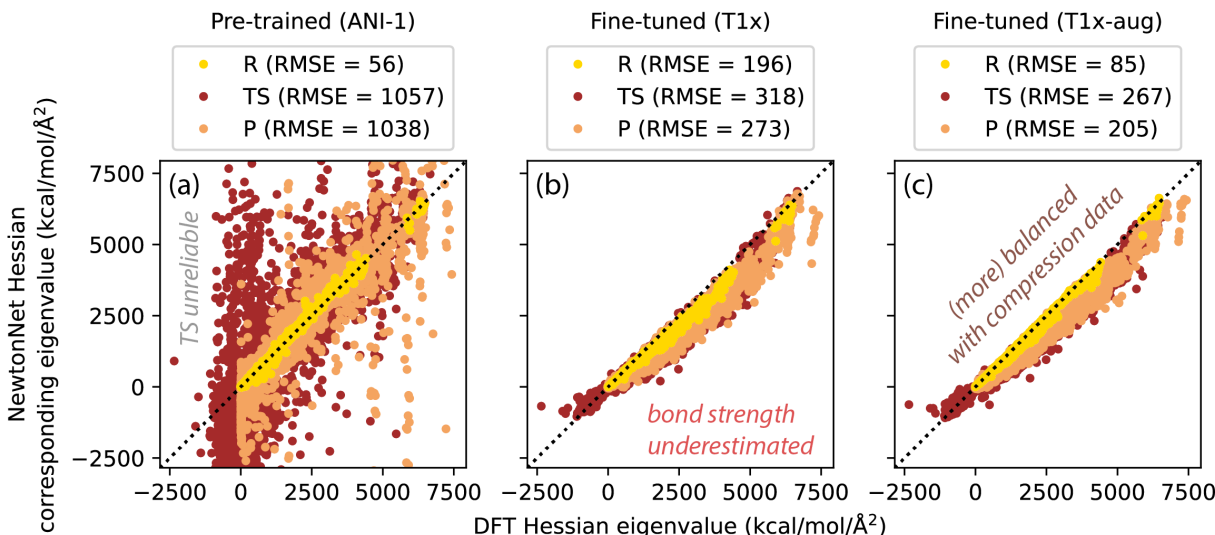


Figure 2: Pre-trained and fine-tuned NewtonNet eMPNN performance on Hessian prediction of the test set. (a) The pre-trained model accurately predicts Hessians at reactant R and product P minima geometries but fails dramatically at TSs. (b) The fine-tuned model using the T1x data significantly improves the accuracy at TSs but with notable underestimation of Hessian eigenvalues. (c) Augmenting the T1x dataset with compressed bond configurations creates a more balanced training data and improves the overall performance. More comprehensive comparisons of the pre-trained and fine-tuned ML prediction accuracy for Hessians is provided in Supplementary Figs. S4-S8.

2.2 Transition State Optimization using Machine Learned Hessians

The fine-tuned NewtonNet model for predicting TS properties is subsequently employed in practical TS optimization scenarios involving new reactions independent of the augmented ANI-1X/T1x training and test data. These include hydrogen migration reactions, endo- and exo-cyclization, generalized Korcek step 2 reactions, retro-ene reactions, and reverse 1,2 and 1,3 insertions (see Supplementary Figs. S9-S12); given the training data these involve only closed-shell molecules. We focus on TS optimization for these unseen reactions in order to compare a traditional QN method that approximates Hessians using gradient information from DFT calculations or ML predictions versus a full explicit ML Hessian used at every step.

We interfaced our fine-tuned NewtonNet model with Sella, a state-of-the-art open source TS geometry optimizer.³⁸ In Sella, the interconversion between the Cartesian coordinates and the redundant internal coordinates is automatically handled, and the Hessian is iteratively diagonalized for the leftmost eigenvector¹⁰ used in the geodesic saddle point optimization.⁴⁶ In order to start the TS optimization for the 240 Sella benchmark reactions, we generated initial guesses with KinBot using reaction templates,³⁷ where each template also defines the intended reactant and product end states for a given reaction. We employed

restricted step partitioned rational function optimization (RS-PRFO)^{47–49} for the TS optimizations, with dynamically adjusted step sizes determined by evaluating the confidence of each step (see Methods for details). After TS optimization, we follow the intrinsic reaction coordinate (IRC) from the optimized TS structure to find the minimum energy path that connects the reactant and product; the robustness of the TS optimization methods is quantified by comparing the intended reactions and the predicted reactions. The complete list of found transition states of the 240 predicted benchmark reactions is summarized in Supplementary Table S1.

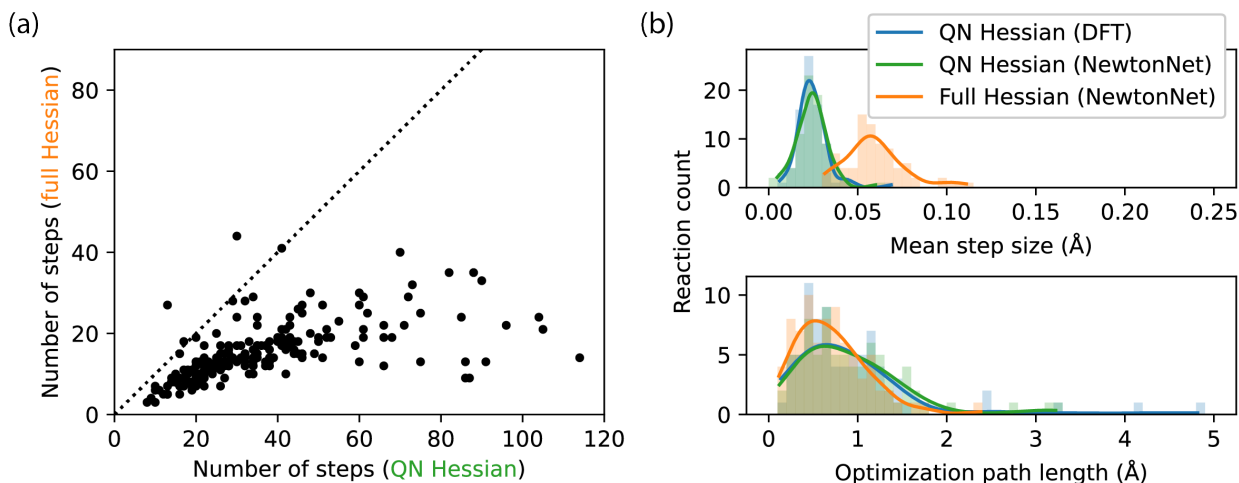


Figure 3: Efficiency improvement using full-Hessian TS optimization compared to the quasi-Newton approach. (a) The full-Hessian TS optimization requires 50% fewer steps to reach convergence than the QN approximate-Hessian approach, using the identical NewtonNet force field on the same reactions. (b) The improved efficiency of the full-Hessian TS optimization comes from both more confident steps (top) and more direct paths (bottom) to converge. In this efficiency comparison, exploration steps of initial Hessian construction or Hessian re-construction for QN restarts have been excluded, whether using DFT or NewtonNet for gradient calculations.

Figure 3 shows how optimization efficiency is dramatically improved by providing full explicit Hessians at every optimization step, which is now affordable relative to DFT as illustrated in Supplementary Figure S13. In Figure 3(a) we find that the number of steps required to converge to a TS can be reduced by 2× of that required by the QN approach using the ML (or DFT; see Supplementary Figure S14). The trend is notably non-linear, and full-Hessian optimization is even more advantageous for challenging tasks that require larger numbers of optimization steps. If the iterative diagonalization steps for initial Hessian construction and Hessian reconstruction when the QN approximation breaks down are included, a reduction of close to 3× of the required steps is observed when considering these gradient calls. Greater optimization efficiency can stem from two factors: increased confidence at each optimization step to increase the step size and a more optimal overall path of optimization. As shown in Figure 3(b), both factors improve the efficiency of the TS optimization with full analytical Hessians. In particular use of the full analytical Hessians exhibits an increase in confidence as measured by the RS-PRFO method, which allows for increased step size on average. A shorter, closer to optimal optimization path also plays a smaller but significant role with the analytical Hessians compared to the QN approaches whether on the ML or DFT PES.

Next we consider the robustness of TS optimization using the fully analytical Hessians versus approximate Hessians (using ML or DFT) by comparing the intended reactions from KinBot to those predicted from the IRC after TS optimization. As shown in Figure 4(a), the NewtonNet full or QN Hessian yielded the intended IRC reactant and product endpoints (2-end match) more often than the QN Hessian from DFT. In some cases only a 1-end match is found because the predicted product is more stable, and more chemically plausible, than the intended product from KinBot. We also characterize the types of TSs found

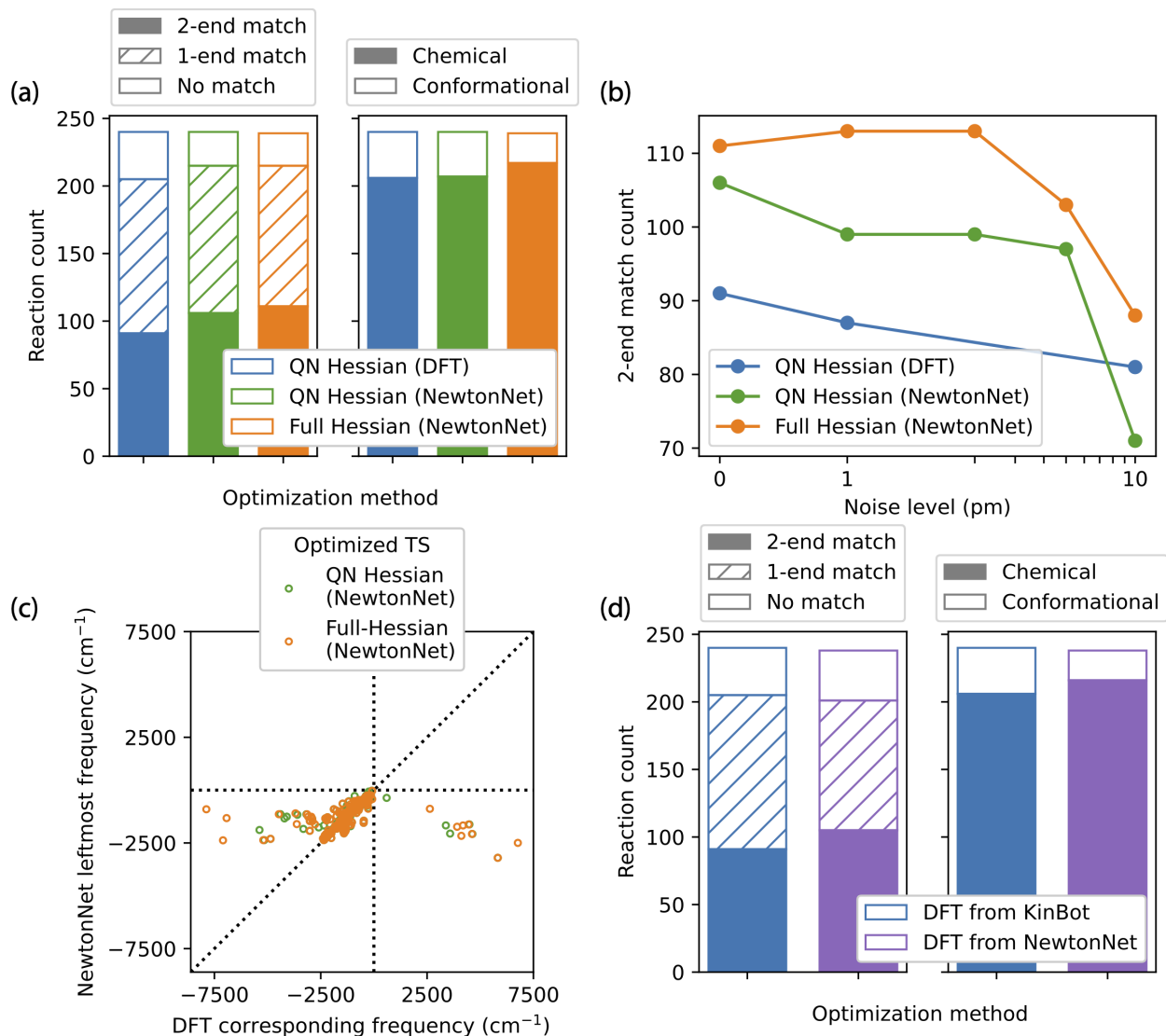


Figure 4: *The quality of optimized TSs using NewtonNet.* (a) NewtonNet predicts reactions that match the intended reactions with higher success rates, both with and without full Hessians, compared to DFT. The full Hessian also finds $\sim 10\%$ more TSs which involve chemical reactions as opposed to conformational changes. (b) The value of the full Hessians over the approximate QN approaches is apparent when the quality of the initial TS guesses deteriorates. The QN convergence decays with additional noise to the guess structures, while the full Hessian convergence is more robust to perturbations. (c) Comparing whether the left most frequency found on the ML PES is also a negative frequency on the DFT PES using the ML geometry. (d) Reoptimizing the ML transition state structure on the DFT surface demonstrates superior performance for 2-end matches and identifying chemical reactions compared with starting from the original KinBot initial guess.

in Figure 4(a), in which the graphs of the reactants and products are inequivalent for chemical reactions, whereas isomorphic endpoints indicate a conformational TS; in either case, both converge to a first-order saddle point. All KinBot initial guess geometries are intended to yield chemical reaction TSs, and we see that employing full Hessians in TS optimization yields $\sim 10\%$ more TSs that involve chemical reactions as opposed to conformational changes compared to the approximate QN method.

The unreliability of a generated initial guess structure can lead to poor convergence or inaccurate predictions. Therefore, we consider a measure of robustness in which the TS optimization must recover from a poor starting structure, which we analyze by systematically introducing random structural perturbations to the guess structures generated from KinBot. Figure 4(b) demonstrates the robustness of NewtonNet’s full-Hessian optimization, maintaining consistent performance and even exhibiting slight improvements as noise levels increase up until 2–3 pm, unlike the QN methods. In contrast, the performance using approximated QN Hessians rapidly decays, even using DFT, highlighting the importance of accurate Hessians for robust TS optimization.

A final important metric of robustness is whether NewtonNet predicted TS structures have negative eigenvalues on the DFT PES and/or improve the outcome of TS optimization on the DFT PES. In Figure 4(c) we compare the vibrational frequencies of the NewtonNet optimized TS saddle point structures, using both the full Hessian and the QN Hessian, and use those structures as input to calculate the frequencies from the DFT Hessian. We then identify the DFT frequency mode that corresponds to the negative frequency mode from NewtonNet. For $\sim 96\%$ of the reactions, NewtonNet predicts highly accurate imaginary frequencies, regardless of full or QN Hessians. However, there are 10 cases for the QN-ML saddle points, and 11 for the full-ML Hessian saddle points, which have positive DFT Hessian eigenvalues. We further reoptimized all 240 reactions using the full Hessian ML TS structures as initial guesses on the DFT surface (Figure 4(d)). In comparison with the optimization outcomes when starting with the original KinBot guess structures, we see an increase in both 2-end matches and chemical transformations under the DFT reoptimization. Thus, starting from ML optimized TS structures we find overall improved solutions on the DFT surface.

3 Conclusion

We have presented a highly generalizable approach for predicting ab initio Hessians using machine learning based solely on energy and gradient data, and only requiring the property of second-order differentiability. Although Denzel and co-workers found that the feasibility of predicting Hessians using ML without access to explicit Hessian training data was poor,³⁵ our study shows that solely relying on energy and force data using a well-trained ML model can efficiently and accurately predict the Hessian for reactive systems. We attribute our contrasting conclusions to the sufficiently high-quality PES obtained through the deep equivariant message-passing neural network and the mathematical relationship between the potential energy and its derivatives using a ML model that is C^2 continuous. To our knowledge, none of the widely used chemical datasets currently include Hessian information, and it is unlikely that such datasets will become available in the foreseeable future due to the high cost of generating ab initio Hessians. Thus, it is good news that models trained on energies and forces are sufficient to derive meaningful ML Hessians.

The ability to generate high-quality explicit Hessians by deep learning models obviates the complexities and assumptions associated with standard TS optimization approaches, in which 240 new reactions never seen in the training data are predicted with greater efficiency, accuracy, and robustness compared to QN ML or DFT. The implementation in Sella to utilize the ML Hessians incurs minimal additional computational overhead and requires no model retraining. Using NewtonNet, the Hessians can be calculated at least three orders of magnitude faster than the DFT calculation while use of the full ML Hessian takes 2–3 \times fewer steps in the TS optimization compared to the QN approach.

This work emphasizes new TS state search methodology and hence used available training data from

ANI-1, ANI-1X, and T1x that is specialized for applications involving reactive molecular organic systems but at a low-level of DFT and basis set quality. Hence, for accurate predictions it would be desirable to recalculate these data sets at a higher level of theory, likely better density functionals and certainly larger basis sets, in order to predict quantitative barriers. Of course, with appropriate new data sets, we can generalize the ML-Hessian approach for many practical applications for TS optimization in many areas of chemical and material sciences. This is made possible by the tight software integration we have developed for NewtonNet with Sella, and workflows which could be generalized to other relevant systems.

We envision several new areas of TS optimization using the ML approach we have described here. For example, the TS discovery for a reaction using methods such as NEB,^{25,26} QST,²⁷ and GSM²⁸ often turn to local TS optimization methods when a reasonable approximate structure has been obtained.¹⁰ We showed that our ML transition state structures do improve the DFT optimizations. Therefore, a stepwise procedure that integrates mathematical optimization and machine learning to collaboratively achieve TS discovery for chemical reactions should be viable. In addition, since we can accurately calculate vibrational frequencies at the optimized TS structures, molecular free energy can be efficiently derived using the harmonic approximation. Further, since the quadratic correction can be applied at each step throughout the optimization process, it is possible to optimize TS structures on the free energy surface rather than PES, as is extending the feasibility of variational transition state theory (VTST) to larger systems where ab initio vibrational analysis becomes impractical.⁵⁰

4 Methods

4.1 Data preparation

The T1x dataset for training is split in two different ways to assess the accuracy of the model predictions, illustrated in Supplementary Figure S2. The original splitting in the literature is based on molecular compositions. All geometries with the same formula (equilibrium and non-equilibrium) are part of the same training, validation, and test set, leading to minimum data leakage. The error from this splitting can be regarded as the worst-case uncertainty estimation of an unseen configuration for the application on the real system in Figure 1 and 2. On the other hand, we wish to maximize the chemical knowledge from the dataset learned by our model, so a more conventional splitting among molecular conformations is devised to learn the PES of all reactions. Hence in the design of the test set, we ensured that no reaction had both reactant and product pairs found in the training set.

The reference DFT Hessians are performed using Q-Chem 6.0.0,⁵¹ using the ω B97X functional⁴⁰ and 6-31G* basis set⁵² in order to maintain compatibility with the T1x dataset.³⁶ The eigenvalues are assigned based on the cosine similarity between the predicted and reference eigenvectors as a linear sum assignment problem using the Jonker-Volgenant algorithm.⁵³

The performance of the ML-Hessian and ML- and DFT-QN TS optimizations is evaluated by the Sella benchmark dataset.³⁸ The dataset contains 500 small organic molecules between 7 and 25 atoms in configurations that approximate the TS geometries the across reaction families, among which the 240 reactions are closed shell. We regenerate 240 of them with further refinement, in contrast to the original data, in that the guess structures in our work are constrained minima on ab initio PES instead of saddles on semi-empirical PES.³⁶ We also inject Gaussian noise up to 50 pm directly onto the atomic positions in the Cartesian coordinate of the initial guesses in order to degrade them for the purpose of understanding a given methods ability to still find the TS.

4.2 NewtonNet Model and training details

The NewtonNet model with three message passing layers is trained using the same architecture as described in Reference 31. Each node encodes an atomic environment into 128 features initialized by atom types Z_i , and each edge encodes an interatomic distance R_{ij} in 20 radial basis functions with polynomial cutoff of 5 Å.^{44,54} The node features are equivariantly updated with messages from neighboring nodes and edges. The molecular energy \tilde{E} is the sum of all atomic energies \tilde{E}_i ,⁵⁵

$$\tilde{E} = \sum_{i'}^A \tilde{E}_{i'}(\{Z_i\}, \{R_{ij}\}) \quad (1)$$

where atomic energies \tilde{E}_i are predicted from the node features at the final layer and A is the total number of atoms. The predicted atomic forces \tilde{F}_i are calculated as the first derivative of the molecular energy \tilde{E} with respect to atomic positions R_i ,⁵⁶

$$\tilde{F}_i = -\nabla_i \tilde{E} = -\frac{\partial \tilde{E}}{\partial R_i} \quad (2)$$

and the predicted atomic Hessians \tilde{H}_{ij} are further calculated as the second analytical derivatives of the energy,

$$\tilde{H}_{ij} = \frac{\partial^2 \tilde{E}}{\partial R_j \partial R_i} = \frac{\partial^2 \tilde{E}}{\partial R_i \partial R_j} \quad (3)$$

However, only the energy \tilde{E} and forces \tilde{F}_i are trained in the loss function \mathcal{L} ,

$$\mathcal{L} = \frac{\lambda_E}{M} \sum_m^M (\tilde{E}_m - E_m)^2 + \frac{\lambda_F}{M} \sum_m^M \frac{1}{3A_m} \sum_i^{A_m} \|\tilde{F}_{mi} - F_{mi}\|^2 \quad (4)$$

where M is the total number of molecular graphs, which is 8 million for training, 1 million for validation, and 1 million for testing.

We use mini-batch gradient descent algorithm with a batch size of 100 to minimize the loss function using the Adam optimizer⁵⁷ with initial learning rate of 10^{-4} and decay rate of 0.7 on plateau. Fully connected neural networks with sigmoid linear unit (SiLU) nonlinearity⁴³ for all functions were used throughout the message passing layer. The application of smooth activation functions like SiLU is critical because the network has to be at least twice differentiable for Hessian calculations. We take $\lambda_E = 1$ and $\lambda_F = 20$ in the loss function in Equation 4 to put more emphasis on forces for derivative properties, and additional L2 regularization of 10^{-5} is applied on all trainable parameters to further smooth out the potential energy surface. Layer normalization⁵⁸ on the atomic features at every message passing layer is applied for the stability of training. An ensemble of four models is trained on each splitting manner to ensure the reproducibility and reliability of the prediction. Outlier among the 4 predictions is removed if its absolute difference from the closest number compared to the difference from farthest number is larger than the 95% confidence limit of the Dixon Q’s test.³⁹

4.3 Transition state optimization

For the transition state calculations, we use the Quantum Accelerator (QuAcc),⁵⁹ a Python package for high-throughput computations with an easy-to-use interface for Atomic Simulation Environment (ASE)⁶⁰ optimizers. We utilize Sella³⁸ as the ASE optimizer for TS and intrinsic reaction coordinate (IRC) calculations. A new feature to Sella is introduced in this work to provide an external Hessian matrix at each optimization step. Details of the Sella settings are described in the Supplementary Information and

we refer readers to the Sella paper for more information.¹⁰ The comparison of reactants and products are based on graph isomorphism. Molecular connectivity graphs are created using Open Babel⁶¹ with atom indexing and compared using the VF2 algorithm.⁶² The optimization path length is calculated in the Cartesian coordinate with the Kabsch algorithm.⁶³ The path length in Figure 3(b) only accounts ones with 2-end matches.

5 DATA AVAILABILITY

All data⁶⁴ including initial transition state guess structures, optimized transition states, and corresponding reactants and products with their coordinates of geometry, energy, forces and Hessians are available at <https://doi.org/10.6084/m9.figshare.25356616>. Source data for Figures 1-4 is available with this manuscript.

6 CODE AVAILABILITY

The codebase is comprised of several publicly available packages and tools that contribute to the project. Sella³⁸ is publicly accessible at <https://github.com/zadorlab/sella> and comes with comprehensive documentation. NewtonNet⁶⁵, another integral part of the project, is also publicly available at <https://github.com/THGLab/NewtonNet/tree/v1.0.0>. The recipes implemented in QuAcc for NewtonNet and Q-Chem, utilizing Sella as the ASE optimizer for transition state and IRC calculations, are publicly accessible and accompanied by thorough documentation.⁵⁹ Wrappers to QuAcc and Q-Chem, employed for running calculations and storing data in the MongoDB database, are available for NewtonNet at <https://github.com/Quantum-Accelerators/quacc>. The full workflow and the analysis scripts⁶⁶, responsible for generating molecular graphs, retrieving data from the MongoDB database, and performing graph isomorphisms to analyze reactions, are available at <https://github.com/THGLab/MLHessian-TSopt/tree/main>. This comprehensive summary provides insights into the availability of the codebase for potential readers and collaborators.

7 ACKNOWLEDGMENTS

S.M.B., A. K., E.C.-Y.Y., and T.H-G. thank the LBL Laboratory Director Research Development program for the work supporting transition state methods. E.C.-Y.Y., X.G. and T.H-G. thank the CPIMS program, Office of Science, Office of Basic Energy Sciences, Chemical Sciences Division of the U.S. Department of Energy under Contract DE-AC02-05CH11231 for support of the machine learning. A.S.R. acknowledges support via a Miller Research Fellowship from the Miller Institute for Basic Research in Science, University of California, Berkeley. This work used computational resources provided by the National Energy Research Scientific Computing Center (NERSC), a U.S. Department of Energy Office of Science User Facility operated under Contract DE-AC02-05CH11231, and the Lawrence computational cluster resource provided by the IT Division at the Lawrence Berkeley National Laboratory (Supported by the Director, Office of Science, Office of Basic Energy Sciences, of the U.S. Department of Energy under Contract No. DE-AC02-05CH11231).

8 AUTHOR CONTRIBUTIONS STATEMENT

S.M.B. and T.H.G. designed the project. E.C.-Y.Y. and X.G. carried out the NewtonNet training and Hessian calculations, E.H., A.K. and S.M.B. interfaced NewtonNet with the Sella software package, A.K., S.M.B., and A.S.R. implemented workflows, A.K. and S.M.B. executed TS workflows, J.Z. ran KinBot to

generate initial guess structures and reference endpoints, and E.C.-Y.Y. and T.H.G. wrote the paper. All authors discussed the results and made comments and edits to the manuscript.

9 COMPETING INTERESTS STATEMENT

The authors declare no competing interests.

References

- [1] Davidson, E. R. The iterative calculation of a few of the lowest eigenvalues and corresponding eigenvectors of large real-symmetric matrices. *J. Comp. Phys.* **1975**, *17*, 87–94.
- [2] Amos, R. D.; Rice, J. E. Implementation of analytic derivative methods in quantum chemistry. *Comp. Phys. Rep.* **1989**, *10*, 147–187.
- [3] Nelder, J. A.; Mead, R. A Simplex Method for Function Minimization. *Comput. J.* **1965**, *7*, 308–313.
- [4] Brent, R. *Algorithms for Minimization without Derivatives*; Prentice-Hall: Englewood Cliffs, NJ, 1973.
- [5] Debye, P. Näherungsformeln für die Zylinderfunktionen für große Werte des Arguments und unbeschränkt veränderliche Werte des Index. *Math. Ann.* **1909**, *67*, 535–558.
- [6] Hestenes, M. R.; Stiefel, E. Methods of conjugate gradients for solving linear systems. *J. Res. Natl. Bureau Stand.* **1952**, *49*, 409–435.
- [7] Nocedal, J.; Wright, S. J. *Numerical Optimization*, 2nd ed.; Springer: New York, NY, USA, 2006.
- [8] Baker, J. An algorithm for the location of transition states. *J. Comp. Chem.* **1986**, *7*, 385–395.
- [9] Schlegel, H. B. Geometry optimization. *WIREs: Comput. Mol. Sci.* **2011**, *1*, 790–809.
- [10] Hermes, E. D.; Sargsyan, K.; Najm, H. N.; Zádor, J. Accelerated Saddle Point Refinement through Full Exploitation of Partial Hessian Diagonalization. *J. Chem. Theo. Comput.* **2019**, *15*, 6536–6549.
- [11] Császár, P.; Pulay, P. Geometry optimization by direct inversion in the iterative subspace. *J. Mol. Struct.* **1984**, *114*, 31–34.
- [12] Schlegel, H. B. Optimization of equilibrium geometries and transition structures. *J. Comp. Chem.* **1982**, *3*, 214–218.
- [13] Schlegel, H. B. Estimating the hessian for gradient-type geometry optimizations. *Theo. Chim. Acta* **1984**, *66*, 333–340.
- [14] Schlegel, H. B. *Advances in Chemical Physics*; John Wiley & Sons, Ltd, 1987; p 249–286.
- [15] Fischer, T. H.; Almlof, J. General methods for geometry and wave function optimization. *J. Phys. Chem.* **1992**, *96*, 9768–9774.
- [16] Lindh, R.; Bernhardsson, A.; Karlstrom, G.; Malmqvist, P.-A. On the use of a Hessian model function in molecular geometry optimizations. *Chem. Phys. Lett.* **1995**, *241*, 423–428.
- [17] Jensen, F. Using force fields methods for locating transition structures. *J. Chem. Phys.* **2003**, *119*, 8804–8808.

- [18] Chantreau Majerus, R.; Robertson, C.; Habershon, S. Assessing and rationalizing the performance of Hessian update schemes for reaction path Hamiltonian rate calculations. *J. Chem. Phys.* **2021**, *155*, 204112.
- [19] Byrd, R. H.; Khalfan, H. F.; Schnabel, R. B. Analysis of a Symmetric Rank-One Trust Region Method. *SIAM J. Opt.* **1996**, *6*, 1025–1039.
- [20] Dennis Jr, J. E.; Schnabel, R. B. *Numerical methods for unconstrained optimization and nonlinear equations*; SIAM, 1996.
- [21] Anglada, J. M.; Bofill, J. M. How good is a Broyden–Fletcher–Goldfarb–Shanno-like update hessian formula to locate transition structures? Specific reformulation of Broyden–Fletcher–Goldfarb–Shanno for optimizing saddle points. *J. Comp. Chem.* **1998**, *19*, 349–362.
- [22] Fletcher, R. *Practical methods of optimization*; John Wiley and Sons, 2000.
- [23] Bofill, J. M. Remarks on the updated Hessian matrix methods. *Int. J. Quant. Chem.* **2003**, *94*, 324–332.
- [24] Hratchian, H. P.; Schlegel, H. B. Using Hessian Updating To Increase the Efficiency of a Hessian Based Predictor-Corrector Reaction Path Following Method. *J. Chem. Theo. Comput.* **2005**, *1*, 61–9.
- [25] Jonsson, H.; Mills, G.; Jacobsen, K. W. *Classical and Quantum Dynamics in Condensed Phase Simulations*; World Scientific, 1998; pp 385–404.
- [26] Henkelman, G.; Uberuaga, B. P.; Jónsson, H. A climbing image nudged elastic band method for finding saddle points and minimum energy paths. *J. Chem. Phys.* **2000**, *113*, 9901–9904.
- [27] Govind, N.; Petersen, M.; Fitzgerald, G.; King-Smith, D.; Andzelm, J. A generalized synchronous transit method for transition state location. *Computational Materials Science* **2003**, *28*, 250–258.
- [28] Peters, B.; Heyden, A.; Bell, A. T.; Chakraborty, A. A growing string method for determining transition states: Comparison to the nudged elastic band and string methods. *J. Chem. Phys.* **2004**, *120*, 7877–7886.
- [29] Zhang, Y.; Wang, H.; Chen, W.; Zeng, J.; Zhang, L.; Wang, H.; E, W. DP-GEN: A concurrent learning platform for the generation of reliable deep learning based potential energy models. *Comp. Phys. Comm.* **2020**, *253*, 107206.
- [30] Bac, S.; Patra, A.; Kron, K. J.; Mallikarjun Sharada, S. Recent Advances toward Efficient Calculation of Higher Nuclear Derivatives in Quantum Chemistry. *J. Phys. Chem. A* **2022**, *126*, 7795–7805.
- [31] Haghightlari, M.; Li, J.; Guan, X.; Zhang, O.; Das, A.; Stein, C. J.; Heidar-Zadeh, F.; Liu, M.; Head-Gordon, M.; Bertels, L.; Hao, H.; Leven, I.; Head-Gordon, T. NewtonNet: a Newtonian message passing network for deep learning of interatomic potentials and forces. *Dig. Disc.* **2022**, *1*, 333–343.
- [32] Duan, C.; Du, Y.; Jia, H.; Kulik, H. J. Accurate transition state generation with an object-aware equivariant elementary reaction diffusion model. *Nature Comp. Sci.* **2023**, *3*, 1045–1055.
- [33] Kim, S.; Woo, J.; Kim, W. Y. Diffusion-based generative AI for exploring transition states from 2D molecular graphs. *Nature Comm.* **2024**, *15*, 341.
- [34] Denzel, A.; Kästner, J. Gaussian Process Regression for Transition State Search. *J. Chem. Theo. Comput.* **2018**, *14*, 5777–5786.

- [35] Denzel, A.; Kästner, J. Hessian Matrix Update Scheme for Transition State Search Based on Gaussian Process Regression. *J. Chem. Theo. Comput.* **2020**, *16*, 5083–5089.
- [36] Schreiner, M.; Bhowmik, A.; Vegge, T.; Busk, J.; Winther, O. Transition1x - a dataset for building generalizable reactive machine learning potentials. *Scientific Data* **2022**, *9*, 779.
- [37] Van de Vijver, R.; Zádor, J. KinBot: Automated stationary point search on potential energy surfaces. *Comp. Phys. Comm.* **2020**, *248*, 106947.
- [38] Hermes, E. D.; Sargsyan, K.; Najm, H. N.; Zádor, J. Sella, an Open-Source Automation-Friendly Molecular Saddle Point Optimizer. *J. Chem. Theo. Comput.* **2022**, *18*, 6974–6988.
- [39] Guan, X.; Heindel, J. P.; Ko, T.; Yang, C.; Head-Gordon, T. Using machine learning to go beyond potential energy surface benchmarking for chemical reactivity. *Nature Comp. Sci.* **2023**, *3*, 965–974.
- [40] Chai, J.-D.; Head-Gordon, M. Systematic optimization of long-range corrected hybrid density functionals. *J. Chem. Phys.* **2008**, *128*, 084106.
- [41] Smith, J. S.; Isayev, O.; Roitberg, A. E. ANI-1: an extensible neural network potential with DFT accuracy at force field computational cost. *Chem. Sci.* **2017**, *8*, 3192–3203.
- [42] Smith, J. S.; Nebgen, B.; Lubbers, N.; Isayev, O.; Roitberg, A. E. Less is more: Sampling chemical space with active learning. *J. Chem. Phys.* **2018**, *148*, 241733.
- [43] Elfving, S.; Uchibe, E.; Doya, K. Sigmoid-weighted linear units for neural network function approximation in reinforcement learning. *Neural Networks* **2018**, *107*, 3–11.
- [44] Gasteiger, J.; Groß, J.; Günnemann, S. Directional Message Passing for Molecular Graphs. **2022**, arXiv:2003.03123 [physics, stat].
- [45] Sharada, S. M.; Bell, A. T.; Head-Gordon, M. A finite difference Davidson procedure to sidestep full ab initio hessian calculation: Application to characterization of stationary points and transition state searches. *J. Chem. Phys.* **2014**, *140*, 164115.
- [46] Hermes, E. D.; Sargsyan, K.; Najm, H. N.; Zádor, J. Geometry optimization speedup through a geodesic approach to internal coordinates. *J. Chem. Phys.* **2021**, *155*, 094105.
- [47] Banerjee, A.; Adams, N.; Simons, J.; Shepard, R. Search for stationary points on surfaces. *J. Phys. Chem.* **1985**, *89*, 52–57.
- [48] Anglada, J. M.; Bofill, J. M. A reduced-restricted-quasi-Newton–Raphson method for locating and optimizing energy crossing points between two potential energy surfaces. *J. Comp. Chem.* **1997**, *18*, 992–1003.
- [49] Besalú, E.; Bofill, J. M. On the automatic restricted-step rational-function-optimization method. *Theo. Chem. Acc.* **1998**, *100*, 265–274.
- [50] Bao, J. L.; Truhlar, D. G. Variational transition state theory: theoretical framework and recent developments. *Chem. Soc. Rev.* **2017**, *46*, 7548–7596.
- [51] Epifanovsky, E. et al. Software for the frontiers of quantum chemistry: An overview of developments in the Q-Chem 5 package. *J. Chem. Phys.* **2021**, *155*, 084801.

- [52] Ditchfield, R.; Hehre, W. J.; Pople, J. A. Self-Consistent Molecular-Orbital Methods. IX. An Extended Gaussian-Type Basis for Molecular-Orbital Studies of Organic Molecules. *J. Chem. Phys.* **2003**, *54*, 724–728.
- [53] Crouse, D. F. On implementing 2D rectangular assignment algorithms. *IEEE Transactions on Aerospace and Electronic Systems* **2016**, *52*, 1679–1696.
- [54] Schütt, K. T.; Unke, O. T.; Gastegger, M. Equivariant message passing for the prediction of tensorial properties and molecular spectra. *Proceedings of the 38th International Conference on Machine Learning* **2021**, *139*, 9377–9388.
- [55] Behler, J.; Parrinello, M. Generalized Neural-Network Representation of High-Dimensional Potential-Energy Surfaces. *Phys. Rev. Lett.* **2007**, *98*, 146401.
- [56] Chmiela, S.; Sauceda, H. E.; Müller, K.-R.; Tkatchenko, A. Towards exact molecular dynamics simulations with machine-learned force fields. *Nature Comm.* **2018**, *9*, 3887.
- [57] Kingma, D. P.; Ba, J. Adam: A Method for Stochastic Optimization. **2017**, arXiv:1412.6980 [cs].
- [58] Ba, J. L.; Kiros, J. R.; Hinton, G. E. Layer Normalization. **2016**, arXiv:1607.06450 [cs, stat].
- [59] Rosen, A. quacc – The Quantum Accelerator. 2023; <https://github.com/Quantum-Accelerators/quacc>.
- [60] Larsen, A. H. et al. The atomic simulation environment—a Python library for working with atoms. *J. Phys.: Cond. Matt.* **2017**, *29*, 273002.
- [61] O’Boyle, N. M.; Banck, M.; James, C. A.; Morley, C.; Vandermeersch, T.; Hutchison, G. R. Open Babel: An open chemical toolbox. *J. Cheminform.* **2011**, *3*, 33.
- [62] Foggia, P.; Sansone, C.; Vento, M. An Improved Algorithm for Matching Large Graphs. 2001.
- [63] Kabsch, W. A solution for the best rotation to relate two sets of vectors. *Acta Cryst. Sec. A* **1976**, *32*, 922–923.
- [64] Yuan, E.; Kumar, A.; Guan, X.; Hermes, E. D.; Rosen, A.; Zador, J.; Blau, S.; Head-Gordon, T. Data for deep learning of Ab Initio Hessians for transition state optimization. 2024; <https://doi.org/10.6084/m9.figshare.25356616.v1>.
- [65] Yuan, E.; Haghghatlari, M.; Rosen, A. S.; Guan, N. X.; Li, J.; Head-Gordon, T. THGLab/newtonnet: V0.1.0. 2024.
- [66] Yuan, E.; Kumar, A.; Guan, X.; Hermes, E. D.; Rosen, A.; Zador, J.; Blau, S.; Head-Gordon, T. THGLab/mlhessian-tsopt: V1.0.1. 2024; <https://zenodo.org/doi/10.5281/zenodo.10799018>.